Heliyon 10 (2024) e38283

Contents lists available at ScienceDirect

Heliyon

journal homepage: www.cell.com/heliyon

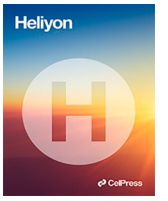

Research article

Preparation, process optimisation, stability and bacteriostatic assessment of composite nanoemulsion containing corosolic acid

Haimei Li [a,1], Xinjia Tan [b,1], Liyan Qin [c], Mansour K. Gatasheh [d], Lei Zhang [e], Wenmin Lin [a], Feng Hu [f], Rian Yan [g], Mariam K. Alshammri [d], Yingbin Shen [a,**], Arshad Mehmood Abbasi [h,i,*], Jing Qi [c,***]

[a] School of Life Sciences, Guangzhou University, Guangzhou, 510006, China
[b] Longping Branch, College of Biology, Hunan University, Changsha, 410125, China
[c] School of Pharmacy, Guangxi University of Chinese Medicine, Guangxi, 530200, China
[d] Department of Biochemistry, College of Science, King Saud University, 2455, Riyadh, 11451, Saudi Arabia
[e] College of Forestry and Landscape Architecture, Xinjiang Agricultural University, Urumqi, 830052, China
[f] Guangdong Chubang Food Co., Ltd, Yangjiang, 529500, China
[g] Department of Food Science and Engineering, Jinan University, Guangzhou, 510632, China
[h] Department of Environmental Sciences, COMSATS University Islamabad, Abbottabad Campus, 22060, Abbottabad, Pakistan
[i] University of Gastronomic Sciences of Pollenzo, Piazza V. Emanuele II, I-12042, Bra/Pollenzo, Italy

ARTICLE INFO

Keywords:
Corosolic acid
Nanoemulsion
Process optimisation
Stability

ABSTRACT

Corosolic acid (CA), a pentacyclic triterpenoid, exhibits remarkably low hydrophilicity, restricting its application in aqueous systems. To enhance its hydrophilicity, we optimised nanoemulsion preparation conditions, resulting in a stable corosolic acid nanoemulsion system. By screening the oil phase, surfactant, and cosurfactant, along with investigating the mass ratio of surfactant and cosurfactant and the preparation temperature, we achieved an optimal corosolic acid nanoemulsion. We measured the particle size, polydispersity coefficient, and Zeta potential of the optimised formulation. The nanoemulsion's sustained-release effect, stability, and antibacterial activity were subsequently examined. The optimised formulation comprised ethyl oleate, cremophor EL, and Tween 80 (1.5:1), combined with ethanol in a ratio of 1:9:2.25 (w/w/w), and was prepared at 30 °C. This optimised corosolic acid nanoemulsion exhibited uniform particle size distribution, favourable dispersion, and notable slow-release capabilities. Importantly, the nanoemulsion demonstrated exceptional stability. In comparison to the positive control's bacteriostatic zone diameter, it was evident that the CA nanoemulsion (1.06 ± 0.11 mm) and blank nanoemulsion (1.03 ± 0.05 mm) both displayed notable inhibitory activity against *S. aureus*. Our findings established a solid foundation for the potential application of CA nanoemulsion in the

* Corresponding author. Department of Environmental Sciences, COMSATS University Islamabad, Abbottabad Campus, 22060, Abbottabad, Pakistan
** Corresponding author.
*** Corresponding author.
E-mail addresses: lihaimei@gzhu.edu.cn (H. Li), tanxinjia123@qq.com (X. Tan), 2597206029@qq.com (L. Qin), mgatasheh@ksu.edu.sa (M.K. Gatasheh), zlei_xj@sina.com (L. Zhang), 2014400067@e.gzhu.edu.cn (W. Lin), hufeng7979@163.com (F. Hu), yanrian813@126.com (R. Yan), mariamkal7@hotmail.com (M.K. Alshammri), shenybin@gzhu.edu.cn (Y. Shen), amabbasi@cuiatd.edu.pk (A.M. Abbasi), qijingxs@163.com (J. Qi).
[1] These authors contributed equally to this work.

https://doi.org/10.1016/j.heliyon.2024.e38283
Received 2 April 2024; Received in revised form 19 September 2024; Accepted 20 September 2024
Available online 21 September 2024

food, cosmetics, and pharmaceutical industries. However, the application of CA nanoemulsion in real food or drug systems has not been explored yet.

1. Introduction

Diverse types of phytochemicals have been approved to possess functional properties [1]. Corosolic acid (CA), an ursane-type pentacyclic triterpenoid, is primarily found in loquat leaves, hawthorn, *Lagerstroemia speciosa, Schisandra chinensis,* raspberry, *Actinidia deliciosa*, sea buckthorn leaves, and wild black cherry [2–4]. It has anti-inflammatory, anti-bacterial, anti-fungal, anti-obesity, antioxidant, anti-cancerous, and anti-tumour bioactivates and is listed as a nutritional supplement in the United States [5,6]. In addition, CA has been called "phyto-insulin" because of its excellent anti-diabetic properties [7]. Importantly, CA has been reported to have anticancer properties but is not harmful to normal cells [6].

However, as a lipophilic compound, CA do not dissolve well in water, which is a key factor limiting their application in food, cosmetics, and pharmaceuticals [4,8]. Various strategies have been employed to improve the water solubility of compounds, such as structure modification, microencapsulation, and emulsions [9,10], are introduction of amino acid groups into CA that is significantly improve the water solubility and α-glucosidase inhibitory activities of CA. But the organic reagents used in the structural modification process may have potential impact on the application of CA in food. Preparation of nanoemulsions is an important means to improving the water solubility of fat-soluble substances without chemical residues. In recent years, there has been extensive domestic and international research on the use of nanocarrier systems to encapsulate natural compounds. These systems are primarily employed to enhance the water solubility of fat-soluble nutrients, stabilise gastrointestinal transit, and facilitate controlled release within the intestines. The aim is to enhance the bioavailability of nutrients [11–13].

Nanoemulsion is a gel-like dispersion system that is thermodynamically stable with a uniform particle size of 20–200 nm [14]. It is widely utilized in medicines, daily chemicals, food, and other fields and has become the focus of research in recent years [15]. In the field of biomedicine, nano-emulsification technology is introduced to elevate water dispersion, bioavailability, and local drug absorption within organisms [16]. Within the food industry, nanoemulsions find utility in safeguarding bioactive substances from undergoing biochemical reactions with other food constituents, thereby effectively preventing deterioration, and ensuring food quality [17]. A lutein-enriched emulsion-based delivery system was formulated to enhance both the water solubility and chemical stability of lutein [18]. In a study by Jia et al. [19] emulsions were shown to augment water solubility and notably improve the oral bioavailability of silybin. Moreover, Zhao et al. [20] demonstrated that nanoemulsions not only enhanced the water solubility of ursolic acid but also increased its inhibitory efficacy against cervical cancer cells.

To expand the utility of CA, we developed an o/w composite nanoemulsion containing corosolic acid. Notably, no prior reports exist on the preparation of a CA nanoemulsion. Hence, our study aimed to optimise the process of generating a CA nanoemulsion. Initially, we optimised the preparation process of the CA nanoemulsion, which encompassed screening the oil phase, surfactant, and cosurfactant, along with investigating the mass ratio of surfactant and cosurfactant (Km value) and the preparation temperature. Subsequently, the particle size, polydispersity coefficient (PDI), and Zeta potential of the optimal CA nanoemulsion were quantified. Lastly, the study assessed the sustained-release effect, stability, and antibacterial activity of the CA nanoemulsion. These investigations collectively evaluate the potential applications of nanoemulsions for food, cosmetics, and pharmaceuticals.

2. Materials and methods

2.1. Chemicals and reagents

The CA was purchased from Chengdu Manshet Biotech Co., Ltd. (Chengdu, China). Ferulic acid, oleic acid, cremophor EL, sodium dodecyl sulphate, disodium hydrogen phosphate, and anhydrous citric acid were obtained from Shanghai Aladdin Biochemical Technology Co., Ltd. (Shanghai, China). Castor oil, ethyl oleate, and Tween 80 were obtained from Shanghai Yuanye Biotech Co., Ltd. (Shanghai, China). Corn oil was obtained from Guangxi BG Oils and Grains Co., Ltd. (Guangxi, China). Glycerol was purchased from Tianjin Fuyu Fine Chemical Co., Ltd. (Tianjin, China). Glacial acetic acid, hydrogen chloride, and absolute ethanol were obtained from Sinopharm Chemical Reagent Co., Ltd. (Shanghai, China). Glyceryl suberate was purchased from Shanghai Haohong Biological Pharmaceutical Technology Co., Ltd. (Shanghai, China). Methanol was obtained from Thermo Fisher Scientific (China) Co., Ltd. (Shanghai, China). Beef extract, casein peptone, agar, ampicillin sodium, and streptomycin sulphate were obtained from Beijing Solarbio Science & Technology Co., Ltd. (Beijing, China). *Escherichia coli* and *Staphylococcus aureus* were obtained from Shanghai Lumi Technology Co., Ltd. (Shanghai, China).

2.2. Preparation and optimisation of CA nanoemulsion system

2.2.1. Solubility of CA in different excipients

The excess CA was added to 0.1 g of oil phase (corn oil, castor oil, oleic acid, or ethyl oleate), surfactant (Tween 80, Cremophor EL, or glyceryl suberate), or cosurfactant (absolute ethanol or glycerol). First, the solution was mixed with vortex (XW-80A, KYlin-Bell Lab Instruments Ltd., Haimen, China). Second, the solution was shaken at 40 °C and 150 rpm for 1 h under dark conditions. Finally, the solution, which was placed at 20–25 °C for 48 h, was centrifuged at 3000 rpm for 15 min, and then the supernatant was diluted with

methanol. The sample solution was filtered with a 0.45-μM filter membrane, then determined via high performance liquid chromatograph (HPLC) (Waters, Massachusetts, USA) connected with a C18 column (4.6 mm × 250 mm, 5 μm). The detection conditions of CA were as follows: the sample solution of 20 μL was injected into a column that was eluted with methanol (A) and ultra-pure water (B) (containing 1 % acetic acid, v/v) at a ratio of 92:8 (v/v) and flow rate of 1.0 mL/min; the column temperature was maintained at 25 °C; and the detection wavelength was 210 nm. The concentrations of CA in different excipients were determined according to the standard curves.

2.2.2. Compatibility of oil phase and surfactant

Following preliminary screening, castor oil, ethyl oleate, or oleic acid were selected as oil phases, and Tween 80, Cremophor EL, or glyceryl suberate were selected as surfactants. The ratio of oil phase to surfactant was set at 1:9, 2:8, 3:7, 4:6, and 5:5 to evaluate the compatibility of oil phase and surfactant in the nanoemulsion system. Then, 0.1 g of the mixture of oil phase and surfactant at each ratio was transferred to 10 mL of distilled water at 37 °C and then stirred evenly with a magnetic stirrer (JB-3, Leici Chuangyi Instrument Ltd., Shanghai, China). A visual evaluation of the final appearance of the emulsion was performed according to the previous criteria [21], as given in Table 1.

2.2.3. Selection of cosurfactants

Utilising the dripping method as reported earlier [22], we established pseudo-ternary phase diagrams of surfactant/cosurfactant, oil phase, and water phase to select the best cosurfactant. The cosurfactants were preliminarily selected as glycerol and absolute ethanol, and the mixed surfactant was prepared with a fixed mass ratio of surfactant and cosurfactant of 2:1. The different weight ratios of the oil phase and the mixed surfactant were set as 9:1, 8:2, 7:3, 6:4, 5:5, 4:6, 3:7, 2:8, and 1:9. Employing the dripping method, the distilled water was slowly added during magnetic stirring. The mass of each component was recorded when the system was changed from clarification to turbidity or turbidity to clarification. Taking the mass fraction of the oil phase, water phase, and mixed surfactant as data points, the pseudo-ternary phase diagram was drawn by Origin 2018 to determine the emulsification region of nanoemulsion. Autodesk AutoCAD 2014 was used to calculate the proportion (area ration) of nanoemulsion in the total area of the three-phase diagram and the minimum dilutable ratio (DR: mass ratio of surfactant and oil phase corresponding to the dilutable line in the pseudo-ternary phase diagram).

2.2.4. Selection of surfactants

The function of surfactants is to reduce the interfacial tension (IFT) between two phases. The reduction of IFT promotes emulsification [23,24]. To screen out the surfactants that conform to the emulsification system, glyceryl suberate, Tween 80, and Cremophor EL were preliminarily selected. Next, we explored the appropriate mass ratios of Tween 80 and Cremophor EL (1:1, 1.5:1, 2:1, 3:1, and 4:1). The mixed surfactants were mixed with absolute ethanol at a ratio of 2:1. The oil phase and the mixture of surfactant and cosurfactant were accurately weighed according to the different proportions (9:1, 8:2, 7:3, 6:4, 5:5, 4:6, 3:7, 2:8, and 1:9) and uniform mixing in a beaker. After accurately weighing the mass of each phase, a pseudo-ternary phase diagram was drawn according to "*2.2.3*" to determine the area ratio of the nanoemulsion, and the cosurfactant according to the maximum area ratio of the nanoemulsion area.

2.2.5. Effect of Km value on nanoemulsion system

The Km value is the mass ratio of surfactant to cosurfactant. The Km values were set as 1, 2, 2.5, 3, and 4. The different weight ratios of oil to mixed surfactant were set as 9:1, 8:2, 7:3, 6:4, 5:5, 4:6, 3:7, 2:8, and 1:9. After accurately weighing the corresponding mass, a pseudo-ternary phase diagram was drawn according to "*2.2.3*" to determine the emulsification area of the nanoemulsion and to calculate the emulsion area ratio and DR of each nanoemulsion.

2.2.6. Effect of preparation temperature on emulsification area, particle size, PDI, and Zeta potential of nanoemulsion

We assessed the effects of different temperatures on the emulsification area and particle size of nanoemulsions using the dripping method [25]. The pseudo-ternary phase diagram was drawn under constant temperatures of 30, 40, and 50 °C, whereby the emulsification area of each nanoemulsion was calculated. The nanoemulsion was diluted 100-fold to prepare an aqueous solution at various preparation temperatures. The impact of different preparation temperatures on particle size, PDI, and Zeta potential was examined. The smaller the PDI of the nanoemulsion, the more homogeneous the system, and the larger the Zeta potential, the better the stability.

2.3. Preparation of CA nanoemulsion under optimised conditions

According to the results of the optimised experiment, 1 mg of CA and 12 mg of ferulic acid were embedded as core materials. Weigh

Table 1
Visual evaluation grade of the compatibility of oil phase and surfactants.

Grade	Appearance
I	emulsion formed, appearing as a clear or slightly bluish solution (A fast, B slow)
II	forming bright white milk with a similar appearance to cow's milk (A with significant stratification, B without stratification)
III	forming a light grey emulsion (A with obvious layering, B without layering)
IV	poorly or minimally emulsified and with large oil globules on the surface

1 g of the oil phase and mix the selected surfactant and cosurfactant were mixed according to the optimum Km of 4 and stirred at a constant speed using the dripping method at 30 °C. The CA nanoemulsion was obtained when the mixture system became clear and transparent. The nanoemulsion was stored at room temperature for future experimentation.

2.4. Determination of the particle size distribution of nanoemulsion

The aqueous solution at 1:100 (w/w) of CA nanoemulsion was prepared. Then, the particle size, PDI, and Zeta potential distribution of the aqueous solution were measured using the Malvern Nanoparticle Size Potential Analyzer (Zse, Malvern Instruments Ltd., California, UK). Each sample was measured thrice at 25 °C.

2.5. Determination of the stability of CA nanoemulsion

2.5.1. Centrifugal stability

The stability of nanoemulsions under centrifugation reflects the emulsion resistance and the integrity of the interfacial film [26,27]. An appropriate volume of the prepared CA nanoemulsion was subjected to centrifugation at varying speeds (3000, 5000, and 8000 r/min) for 30 min, and the presence of stratification was observed. The non-stratified emulsion was assessed for absorbance at 210 nm before and after centrifugation, using distilled water as the blank control. Each measurement was conducted in triplicate, and transmittance was subsequently calculated.

$$\text{Transmittance formula}: T\,(\%) = A1/A2 \times 100 \quad \text{Eq. 1}$$

T: light transmittance; A1: absorbance of nanoemulsion before centrifugation; A2: absorbance of nanoemulsion after centrifugation.

2.5.2. Thermal stability

The thermal stability was performed the previously described method with minor modifications [28]. The prepared CA nanolotion was heated at varying temperatures (40, 50, 60, 70, 80, and 90 °C) for 30 min, and the state of the CA nanoemulsion was observed. The absorbance of the nanoemulsion was measured at 210 nm both before and after heating, with distilled water serving as the blank control. Additionally, the particle size was determined, and the light transmittance was calculated using the formula given in Eq. (1).

2.5.3. pH stability

The pH stability was measured according to the method described by Shi et al. [29]. Considering that our dietary system is almost neutral and acidic, and that the pH of the gastrointestinal tract is also acidic and neutral, we chose pH values of 3.0, 5.0, and 7.0 to test the pH stability of nanoemulsion. Disodium hydrogen phosphate and anhydrous citric acid were used to prepare buffers with pH values of 3.0, 5.0, and 7.0. CA nanoemulsion was prepared using a buffer solution with varying pH values instead of distilled water. We calculated the emulsifying area of the nanoemulsion according to the method described in *2.2.3*. An appropriate volume of the nanoemulsion was subjected to centrifugation at 3000 r/min for 30 min, followed by observation for any signs of stratification in the lotion. The non-stratified lotion was then subjected to absorbance measurements at 210 nm both before and after centrifugation, using distilled water as the blank control. The light transmittance was calculated according to given in Eq. (1).

2.5.4. Storage stability

Nanoemulsion storage stability was measured with reference to previously methods with slight modifications [30,31]. The nanoemulsion was stored in incubators at 4 °C and 25 °C, respectively. The particle size, PDI, and Zeta potential of the CA nanoemulsion were measured on day 1, 7, 14, 21, 39, and 60.

2.6. Determination of drug loading capacity of CA nanoemulsion

The CA nanoemulsion was diluted with methanol and filtered using a filter membrane of 0.45 μM to form the test solution. Based on the chromatographic conditions described in Section *2.2.1*, the drug loading of CA nanoemulsion was determined via HPLC [32].

2.7. Determination of cumulative in vitro release of CA nanoemulsion

The prepared CA nanoemulsion and the same concentration of CA solution were loaded into a dialysis bag with a length of 10 cm (diameter of 18 mm, molecular retention: 2kD) using the dialysis bag method. Then, the dialysis bag with samples was put into a 1 % SDS solution (the dissolution medium). The volume ratio of the sample in the dialysis bag to the dissolution medium was 1:10, the temperature was 37 °C, and the rotating speed was 100 rpm. The release medium of 1 mL was extracted at 1, 2, 3, 4, 6, and 8 h and supplemented with the same volume of fresh release medium [33]. HPLC was used to determine the content of CA in the release medium [34]. The flow rate of the mobile phase was set to 0.6 mL/min. Other HPLC conditions followed those described in Section

2.2.1. The concentrations of CA were determined according to the standard curves.

2.8. Determination of antibacterial activity of CA nanoemulsion

The antibacterial activity of CA nanoemulsion was evaluated using disk diffusion assay as previously described, with slight modifications [26,35]. We selected *E. coli* and *S. aureus* as representatives of gram-negative and gram-positive bacteria, respectively. They were employed to assess the antibacterial efficacy of the CA nanoemulsion. A bacteria suspension of 100 μL (concentration: 1–2 $\times 10^8$) was placed into a culture medium formulated with beef extract, sodium chloride, casein peptone, and agar (0.3:0.5:1:2), and uniformly spread using a coating rod. Filter papers (6 mm) containing the sample, blank control, and positive control were affixed onto the medium's surface, ensuring complete contact with the agar. Subsequently, the cultures were incubated at 37 °C for 24 h. The resulting diameter of the bacteriostatic circles was measured to assess the extent of inhibition. Each group underwent triplicate replication. Group A represented the synergistic CA nanoemulsion with a water content of 90 %, while Group B denoted the blank nanoemulsion with a water content of 90 %. Groups C and D constituted the positive controls, encompassing 0.5 mg/mL penicillin solution and 0.5 mg/mL streptomycin solution.

2.9. Statistical analysis

The experiments were conducted in triplicate, and the results are reported as means ± standard deviations. One-way analysis of variance and independent sample t-tests were performed to compare differences between samples. Statistical analyses were performed using SPSS 16.0. Differences were considered statistically significant at $p < 0.05$.

3. Results and discussion

3.1. Construction and optimisation of CA nanoemulsion

3.1.1. Solubility of CA in different excipients

Suitable oil phase, emulsifier and coemulsifier are critical for the development of CA with poor water solubility. In this study, several oil phases (corn oil, castor oil, oleic acid and ethyl oleate), surfactant (Tween 80, cremophor EL and glyceryl suberate) and cosurfactant (absolute ethanol and glycerol) that have soluble-increasing effect on insoluble ingredients and meet the national food safety standards were selected for evaluation. The dissolution of CA in different solvents was determined by HPLC. Table 1 shows that CA dissolved efficiently in castor oil (23.3822 mg/g) and oleic acid (18.3305 mg/g). However, the solubility of CA in corn oil was only 0.769 mg/g (Table 2). Consequently, corn oil was excluded as the oil phase for the CA nanoemulsion. For emulsifiers, Tween 80 exhibited the highest solubility for CA (41.266 mg/g) compared to Cremophor EL and glyceryl suberate. Among the cosurfactants, CA exhibited better solubility in absolute ethanol (51.5125 mg/g) compared to glycerol. Thus, the subsequent investigation focused on refining selections of oil phases (castor oil and oleic acid), surfactants (Tween 80, Cremophor EL, and glyceryl suberate), and co-surfactants (absolute ethanol and glycerol).

3.1.2. Compatibility of oil phase and surfactant

Except for solubility, the compatibility between the oil phase and emulsifier has an important effect on the emulsifying ability. The poor compatibility between the oil phase and emulsifier will cause the phenomenon of large particle size or delamination [36]. Based on the results of *3.1.1*, different nanoemulsions were prepared using varying mass ratios of oil phases (castor oil, oleic acid, and ethyl oleate) to surfactants (Tween 80, Cremophor EL, and glyceryl suberate) and evaluated visually. The results (Table 3) indicate that Cremophor EL and Tween 80 have good compatibility with the selected three oil phase, which can generate clear or slightly bluish emulsions with the oil phase (I A- III B). Additionally, with castor oil or oleic acid as the oil phase (I A/II A-III B), with a ratio of 1:9–3:7, Cremophor EL exhibited superior emulsification capabilities compared to Tween 80, and vice versa for oleic acid (III A- III B/II A). However, glyceryl octanoate, acting as a surfactant, led to the formation of large oil globules on the emulsion's surface, regardless of

Table 2
Preliminary screening of oil phase, surfactant and cosurfactant.

	Accessories	Solubility of corosolic acid (mg/g)
Oil phase	Corn oil	0.769 ± 0.008^{i}
Oil phase	Castor oil	23.3822 ± 0.01^{c}
Oil phase	Oleic acid	18.3305 ± 0.003^{d}
Oil phase	Ethyl oleate	1.2078 ± 0.001^{h}
Surfactant	Tween 80	41.266 ± 0.005^{b}
Surfactant	Cremophor EL	12.7973 ± 0.008^{e}
Surfactant	Glyceryl suberate	6.58 ± 0.035^{f}
Cosurfactant	Absolute ethanol	51.5152 ± 0.009^{a}
Cosurfactant	glycerol	2.7921 ± 0.001^{g}

Note: Data represent the mean ± standard deviation (n = 3). Significant differences at $p < 0.01$ are marked as alphabets (a-i).

Table 3
Nanoemulsion state under different oil phase and surfactant mass ratios.

O/S mass ratio	1:9	2:8	3:7	4:6	5:5
Castor oil: Tween 80	III B	II A	II A	IV	IV
Castor oil: Cremophor EL	I A	I A	I A	I A	II A
Castor oil: Glyceryl suberate	IV	IV	IV	IV	IV
Ethyl oleate: Tween 80	I B	I B	I B	I B	II A
Ethyl oleate: Cremophor EL	I B	I B	I B	I B	III B
Ethyl oleate: Glyceryl octanoate	IV	IV	IV	IV	IV
Oleic acid: Tween 80	III A	III A	II A	II A	II A
Oleic acid: Cremophor EL	III B	III B	III B	II A	II A
Oleic acid: Glycerol caprylate	IV	IV	IV	IV	IV

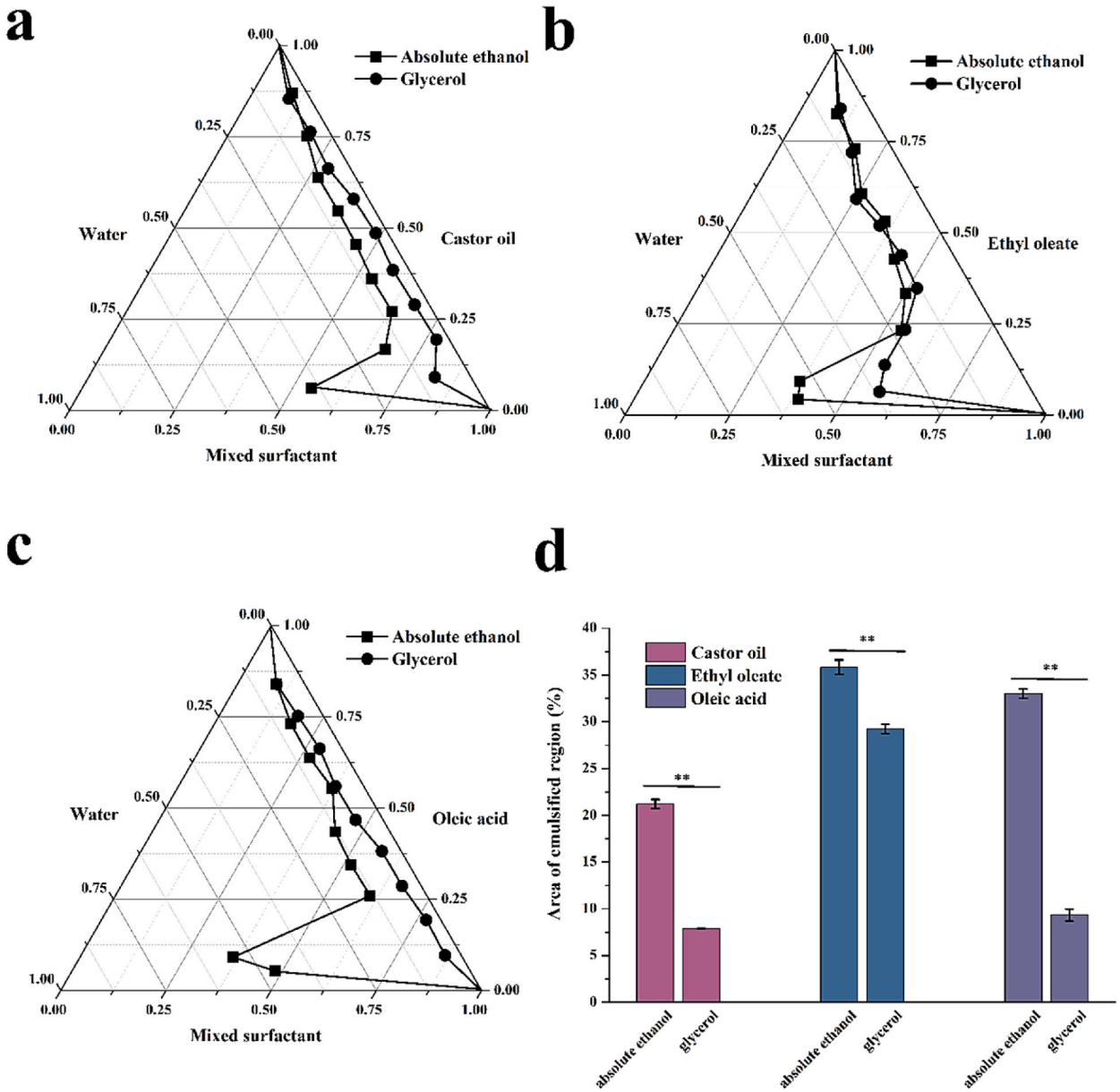

Fig. 1. Ternary phase diagrams of corosolic acid nanoemulsions with different cosurfactants in (a) castor oil, (b) ethyl oleate, (c) oleic acid, and (d) area of the emulsified region of corosolic acid nanoemulsions with three different oil phases by different cosurfactants. Data represent mean ± standard deviation (n = 3). Significant differences ($p < 0.01$) are marked as "**".

the oil phase. Our results are consistent with other studies showing that both Tween 80 and Cremophor EL have excellent emulsifying capabilities when preparing nanoemulsion [35,37]. Therefore, Cremophor EL and Tween 80 were selected as surfactants in subsequent experiments.

3.1.3. Selection of cosurfactants

Coemulsifiers can reduce the amounts of emulsifiers, reduce the irritation to gastrointestinal mucosa, increase the solubility of drugs at the oil or oil-water interface, and increase the micro-emulsion drug load [38]. This study evaluated the effects of glycerol and anhydrous ethanol as emulsifiers. Pseudo-ternary phase diagrams for the different formulations are shown in Fig. 1a–c. The nanoemulsion formulated with glycerol as a cosurfactant displayed poor fluidity, featuring a viscous and pale grey emulsion system with low oil loading that did not align with typical nanoemulsion characteristics. Conversely, the CA nanoemulsion utilising absolute ethanol as a cosurfactant exhibited the most extensive emulsification area, exceptional fluidity, and stability (Fig. 1d). This result signifies that the incorporation of absolute ethanol as a cosurfactant substantially reduced system viscosity and liquid surface tension, enhancing the mobility of the CA nanoemulsion while regulating the distribution of aqueous and oil phases at the interface. Notably, Al-Karaki et al., Zhang et al. and Zhao et al. found that ethanol was the best cosurfactant when studying the selection of emulsifiers [39–41]. Furthermore, absolute ethanol is less irritating to humans. Consequently, absolute ethanol was chosen as the cosurfactant for nanoemulsion preparation.

3.1.4. Selection of surfactants

Studies have shown that the emulsification effect of mixed surfactants is better than that of single surfactants [42]. The results are shown in Fig. 2. The emulsification regions of the nanoemulsion formed by oil phase and the mixed surfactant with DR at 1:9 as follows: The combining castor oil with the mixed surfactant follow the size order: Cremophor EL:Tween 80 (1.5:1) > Cremophor EL:

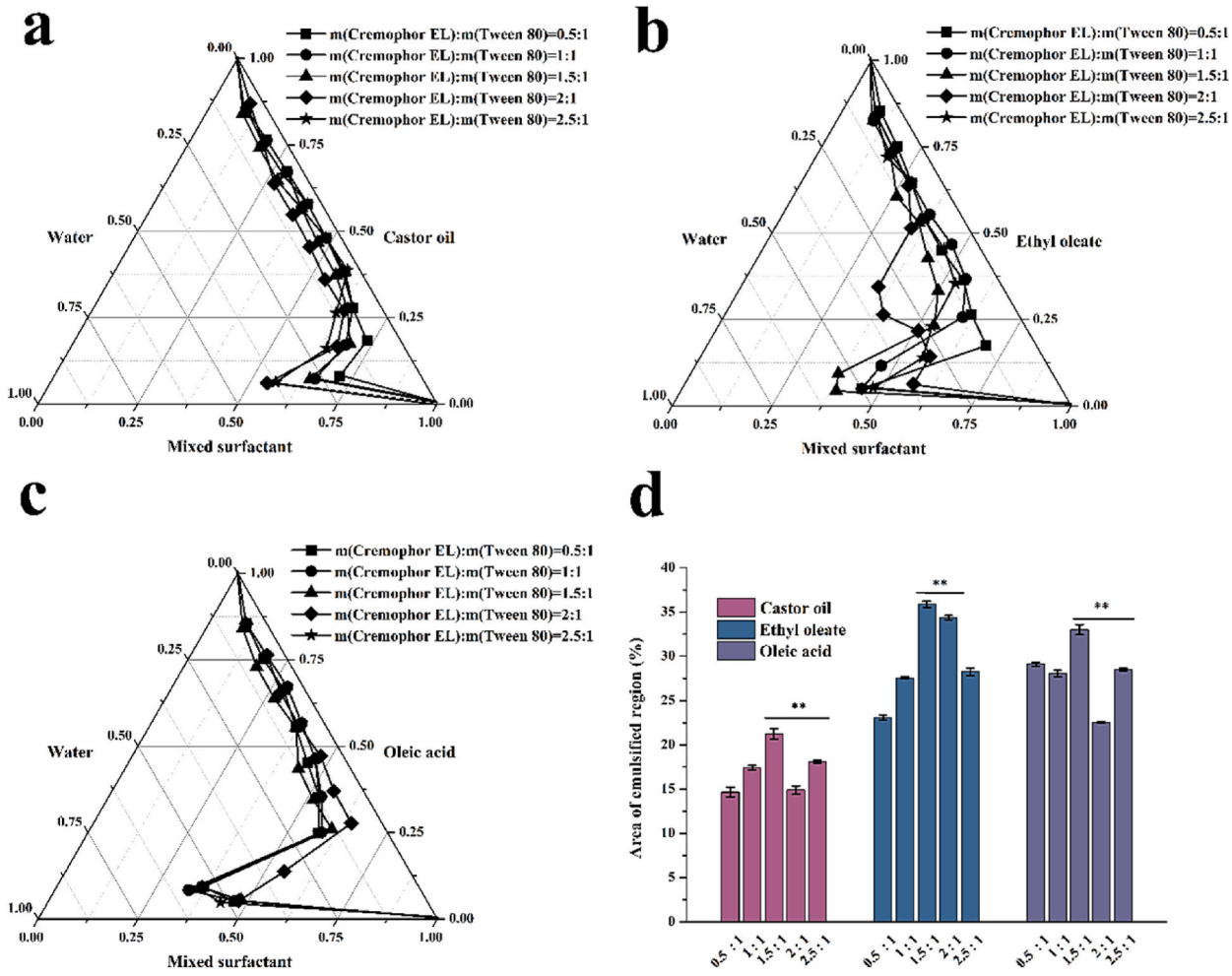

Fig. 2. Ternary phase diagrams of corosolic acid nanoemulsions with different ratios of mixed surfactant in (a) castor oil, (b) ethyl oleate, (c) oleic acid, and (d) the area of the emulsified region of corosolic nanoemulsions with three different oil phases and different ratios of mixed surfactant. Data represent mean ± standard deviation (n = 3). Significant differences ($p < 0.01$) are marked as "**".

Tween 80 (2.5:1) > Cremophor EL:Tween 80 (1:1) > Cremophor EL:Tween 80 (2:1) > Cremophor EL:Tween 80 (0.5:1) (Fig. 2a). The nanoemulsion emulsification regions formed by complexing ethyl oleate with mixed surfactants in the order of area size were Cremophor EL:Tween 80 (1.5:1) > Cremophor EL:Tween 80 (2:1) > Cremophor EL:Tween 80 (2.5:1) > Cremophor EL:Tween 80 (1:1) > Cremophor EL:Tween 80 (0.5:1) (Fig. 2b). The emulsified region area size order of nanoemulsion formed by oleic acid complexed with mixed surfactant was Cremophor EL:Tween 80 (1.5:1) > Cremophor EL:Tween 80 (0.5:1) > Cremophor EL:Tween 80 (2.5:1) > Cremophor EL:Tween 80 (1:1) > Cremophor EL:Tween 80 (2:1) (Fig. 2c). The emulsification area ratios for different oil phases with mixed surfactants at different ratios were calculated using Auto CAD 2014 and the results demonstrates that the formulation with a Cremophor EL:Tween 80 = 1.5:1 leading to the largest emulsification area, suggesting its optimal proportion (Fig. 2d).

3.1.5. Selection of Km values

As shown in Fig. 3a and b and d, the emulsified area of the nanoemulsion consistently increased with increasing Km values when using castor oil and ethyl oleate as the oil phase. When the Km value is small (less than 4), the surfactant content is insufficient, resulting in a relatively small nanoemulsion area. The emulsification area exhibited a clear increasing trend when the Km value reached 4. In contrast, when oleic acid was employed as the oil phase, the emulsified area of the nanoemulsion gradually decreased as the Km value increased. This indicates that a smaller Km value resulted in better fluidity and stability for oleic acid composed nanoemulsion (Fig. 3c and d). The nanoemulsion region's area significantly decreased, along with the reduction in the entrapped oil

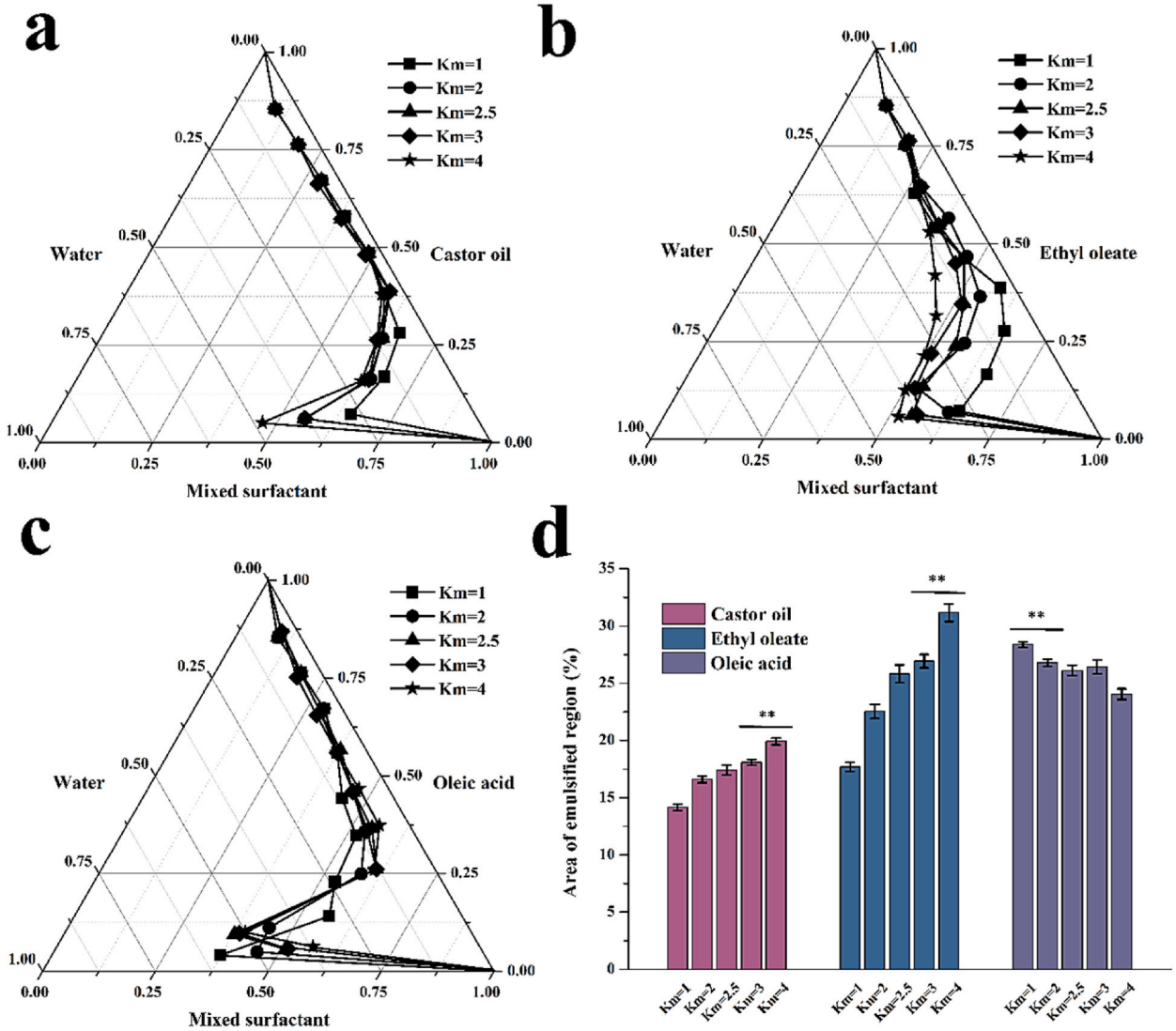

Fig. 3. Ternary phase diagrams of corosolic acid nanoemulsions with different mass ratio of surfactant and cosurfactant (Km value) in (a) castor oil, (b) ethyl oleate, (c) oleic acid, and (d) the area of the emulsified region of corosolic nanoemulsions with three different oil phases with different Km values. Data represent mean ± standard deviation (n = 3). Significant differences ($p < 0.01$) are marked as "**".

phase mass, as the Km value reached 4. Consequently, we chose Km values of 4 for castor oil and ethyl oleate and a Km value of 1 for oleic acid for the subsequent optimisation of the nanoemulsion formulation.

3.1.6. Effect of preparation temperature on nanoemulsion

The results are summarised in Fig. 4 and Table 4. The emulsification area of the nanoemulsion increased with the temperature increasing from 30 to 40 °C for all three different oil phases, then decreased as the temperature reached 50 °C (Fig. 4a, b, 4c). This trend suggests that the reduction in surface tension at 40 °C favoured nanoemulsion formation at the oil-water interface. There was no significant difference in emulsification area between nanoemulsions prepared at 30 °C and 40 °C. The temperature of 30 °C was chosen for subsequent studies due to its closer proximity to ambient temperatures and smaller and more stable particle size and PDI. The oil phase was further screened, revealing that ethyl oleate yielded superior emulsification area and particle size (Table 4). In addition, the PDI value below 0.3 generally indicates a high degree of dispersion uniformity. Thus, ethyl oleate was chosen as the oil phase for the CA nanoemulsion.

3.2. Particle size of CA nanoemulsion under optimised conditions

The droplet size can also have a significant effect on the emulsion stability, viscosity and optical properties [43]. The PDI value indicates the homogeneity and stability of the emulsion's droplet size distribution. PDI values are usually between 0 and 1. The size distribution of the nano-emulsion system is narrow when the PDI is less than 0.3. Under optimised preparation conditions, the CA nanoemulsion exhibited a particle size of 15.47 ± 0.05 nm, a PDI of 0.039 ± 0.002 VM, and a Zeta potential of −1.37 ± 0.90 mV. The nanoemulsion appeared clear-yellowish and displayed transparency with Km value of 4 and preparation temperature of 30 °C, as well as the ethyl oleate as the oil phase, Cremophor EL:Tween 80 = 1.5:1 as surfactants and absolute ethanol as cosurfactants.

3.3. Stability of CA nanoemulsion

3.3.1. Centrifugation stability

The stability of the nanoemulsion is a crucial parameter influencing its properties. In this study, we accelerated potential changes by subjecting the nanoemulsion to centrifugation and evaluating its stability during storage. The absorbance before and after centrifugation in a formulation comprising of 90 % water and 10 % ethyl oleate, surfactant (Cremophor EL:Tween 80 = 1.5:1) and absolute ethanol (1:9:2.25, w/w/w) were measured and calculated light transmittance. The results are shown in Fig. 5a. Visual examination indicated that CA nanoemulsion, centrifuged at different speeds, remained free from turbidity and stratification, maintaining its clarity and transparency with light transmittance exceeding 100 %. This outcome suggests minimal particle aggregation during centrifugation, highlighting the notable centrifugation stability of the CA nanoemulsion.

3.3.2. Thermal stability

The hydrogen bonds within the nonionic surfactants of polyoxymethylene can be disrupted by water at elevated temperatures, causing a rapid decline in surfactant solubility and a shift in the system's appearance from clear to turbid or delaminated. This phenomenon is termed 'transient'. It is of great significance to research the temperature stability, especially for the nanoemulsion system containing many surfactants.

The stability of the nanoemulsion at different temperatures is illustrated in Fig. 5b and c. Based on the aforementioned outcomes, no notable variance in nanoemulsion particle size was observed following various temperature treatments, and the PDI of the

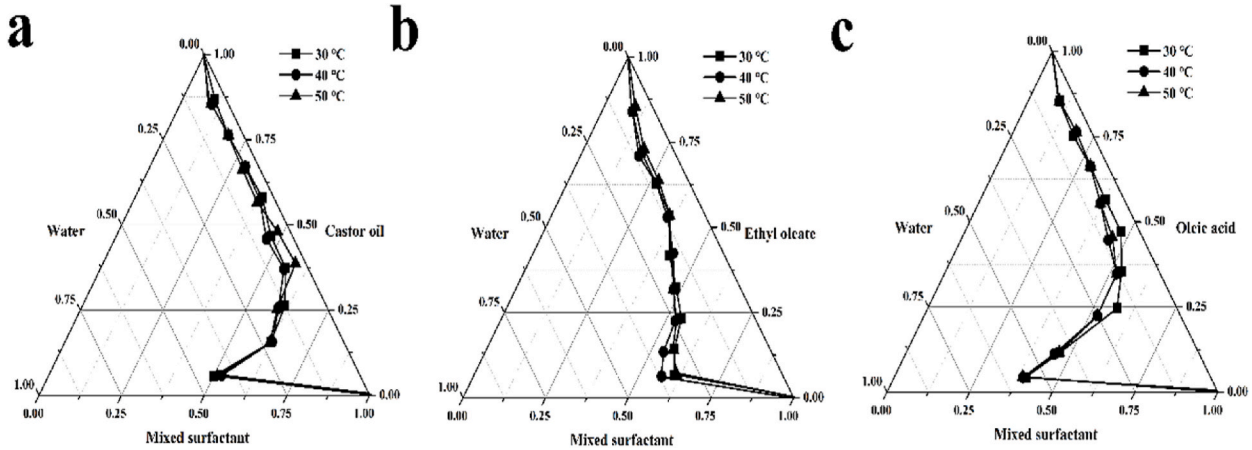

Fig. 4. Ternary phase diagrams of corosolic acid nanoemulsions at different preparation temperatures.

Table 4
Area, mean size, PDI and Zeta potential value of nanoemulsion prepared at different temperatures.

Oil phase	T (°C)	Area (%)	Mean size (nm)	PDI/VM	Zeta potential/mV
Castor oil	30	20.12 ± 0.35^{e}	20.33 ± 0.21^{c}	0.244 ± 0.003^{c}	-6.05 ± 1.045^{b}
	40	21.00 ± 0.46^{e}	14.53 ± 0.13^{d}	0.085 ± 0.013^{e}	-7.17 ± 1.376^{b}
	50	20.22 ± 0.37^{e}	16.46 ± 0.12^{cd}	0.175 ± 0.006^{d}	-5.11 ± 2.165^{b}
Ethyl oleate	30	28.72 ± 0.52^{bc}	14.12 ± 0.03^{d}	0.055 ± 0.001^{e}	-3.36 ± 0.597^{b}
	40	30.58 ± 0.41^{a}	13.95 ± 0.43^{d}	0.082 ± 0.004^{e}	-4.20 ± 2.123^{b}
	50	28.19 ± 0.78^{cd}	17.28 ± 0.28^{cd}	0.217 ± 0.001^{c}	-5.2 ± 2.542^{b}
Oleic acid	30	27.51 ± 0.29^{d}	181.3 ± 0.81^{b}	0.424 ± 0.018^{b}	-28.33 ± 0.472^{a}
	40	30.21 ± 0.66^{a}	267.1 ± 6.71^{a}	0.535 ± 0.032^{a}	-26.77 ± 0.208^{a}
	50	29.76 ± 0.25^{ab}	267.0 ± 0.65^{a}	0.550 ± 0.012^{a}	-26.83 ± 1.001^{a}

Note: Mean size, PDI, and MV average potential of corosolic acid nanoemulsion were determined at 1:9 of O/S. Data represent the mean ± standard deviation (n = 3). Significant differences at $p <$ 0.01 are marked as alphabets (a-e).

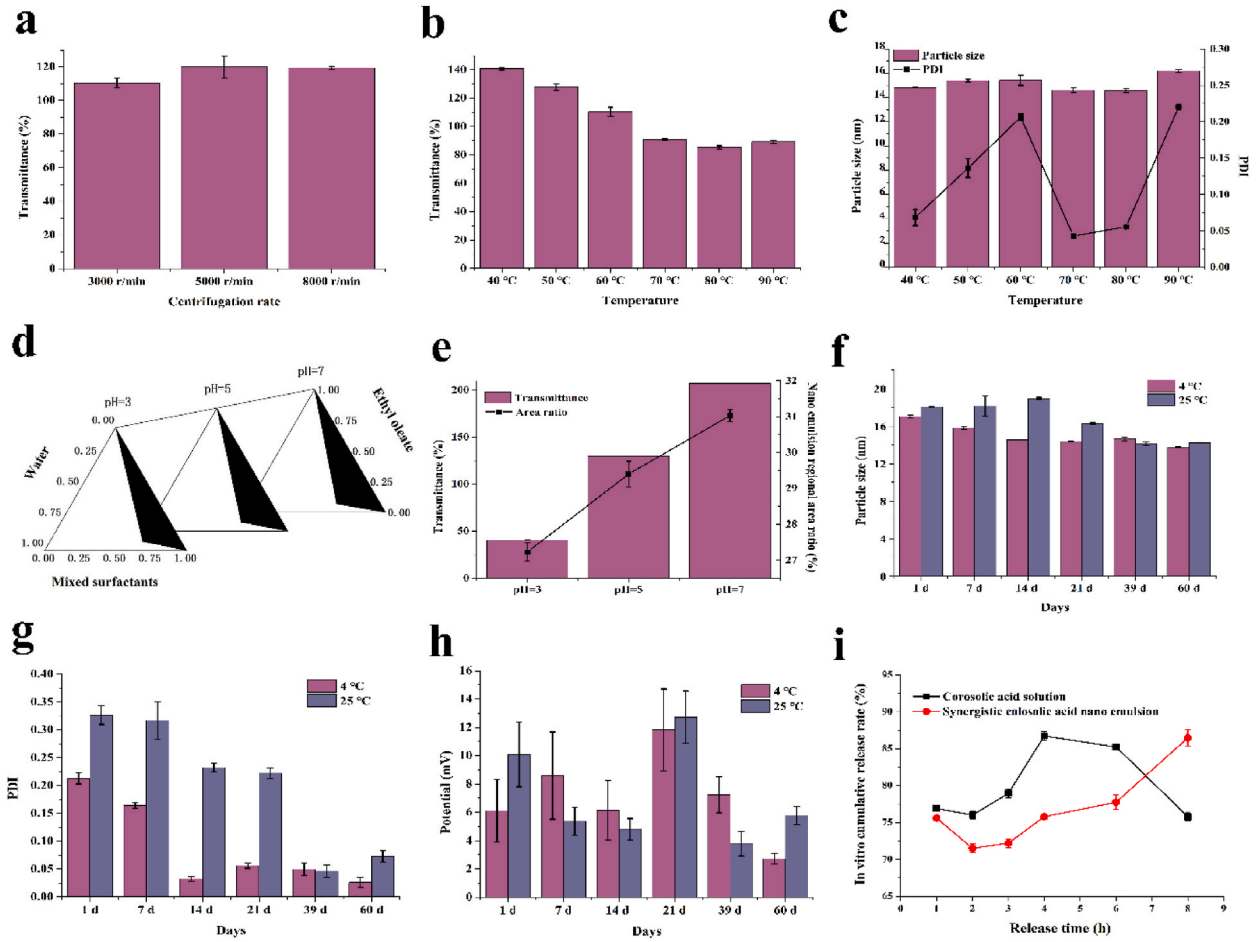

Fig. 5. (a) Transmittance of corosolic acid nanoemulsions at different centrifugation rates; (b) transmittance, (c) particle size, and polydispersity coefficient (PDI) of corosolic acid nanoemulsions at different temperatures; (d) pseudo-ternary phase diagrams, (e) transmittance of corosolic acid nanoemulsions at different pH values; (f) particle, (g) PDI, and (h) potential of corosolic acid nanoemulsions at different storaged under 4 °C and 25 °C; (i) Cumulative release rates in vitro of corosolic acid solution and corosolic acid nanoemulsions.

nanoemulsion remained below 0.3, affirming its commendable uniformity. The nanoemulsion exhibited sustained clarity and transparency, with light permeability exceeding 85 % at emulsion temperatures below 70 °C. The findings indicate the robust thermal stability of this nanoemulsion system up to 70 °C.

3.3.3. pH stability

The pH value of food is typically acidic or neutral. Thus, a buffer solution of acidic and neutral pH was formulated using disodium

hydrogen phosphate and anhydrous citric acid to investigate the effect of pH stability of nanoemulsion. As shown in Fig. 5d and e, an increment in pH corresponds to increased light transmittance and an increased emulsification region area of the nanoemulsion. The results indicate a reduction of approximately 3.80 % in the emulsified area ratio of the nanoemulsion as the pH decreased from 7.0 to 3.0. Furthermore, the light transmittance of the CA nanoemulsion system at pH 3.0 and 5.0 is 40.43 % and 129.83 %, respectively. However, at a pH value of 7.0, the light transmittance reached 207.03 %. This reveals that the CA nanoemulsion system has better stability in neutral conditions than in acidic conditions. Consequently, CA nanoemulsions should be prepared under neutral conditions.

3.3.4. Storage stability

Particle size and PDI are closely linked to the stability of nanoemulsions. Nanoemulsions featuring small particle sizes possess reduced surface tension and enhanced stability. Furthermore, nanoemulsions with diminutive particle dimensions exhibit heightened solubility and bioactivity due to the expanded interfacial surface area, which facilitates drug absorption [44]. A higher degree of surface charge causes droplets of small particle size to repel each other due to the presence of strong intermolecular repulsive forces. This mechanism keeps all charged nanodroplets in a relatively stable Brownian motion [45]. Thus, particle size and PDI constitute pivotal factors influencing nanoemulsion stability.

This study delved into the storage stability of CA nanoemulsion, furnishing insights into its shelf life and storage requirements. The results depicted in Fig. 5f, g, and 5h revealed that particle size and PDI progressively diminished during storage at 4 °C and 25 °C. Notably, the particle size and PDI of nanoemulsions stored at 4 °C were smaller than those stored at 25 °C. This demonstrates that the CA nanoemulsion is more stable at lower temperatures. Furthermore, Zeta potential exhibited its highest absolute value at 4 °C and 25 °C after 21 d of storage, indicating peak electrostatic repulsion among nanoemulsion droplets. In essence, the CA nanoemulsion showcases robust stability at both the low temperature of 4 °C and the ambient temperature of 25 °C.

3.4. Cumulative release in vitro and drug loading assay of the CA nanoemulsion

HPLC was employed to determine the CA content in the medium at various time points. As depicted in Fig. 5i, the CA solution achieved an 86.74 % release rate at 4 h, approaching near-complete release. Conversely, the cumulative release rate of CA from the nanoemulsion within the same timeframe consistently lagged behind that of the CA solution. By the 8-h mark, the CA nanoemulsion exhibited a cumulative release rate of 86.48 %, underscoring its discernible slow-release effect. Moreover, the drug-loading capacity of the CA nanoemulsion reached 0.7345 mg/g, affirming the system's commendable drug-loading efficacy.

3.5. Bacteriostatic activity

The bacteriostatic activity of the compound was assessed by measuring the diameter of the inhibition zone. As indicated in Table 5, the CA nanoemulsion exhibited stronger inhibitory effects against *S. aureus* than those against *E. coli* with an MIC concentration of 1.06 and 0.86 mm, respectively. This disparity can be attributed to the distinct cell envelope structure, with gram-negative bacteria having a double membrane and gram-positive bacteria possessing a single membrane [46]. In addition, the emulsification process may have reduced the hydrophobic property of the CA nano-emulsion, which could increase its antibacterial impact on Gram-positive bacteria [47]. Hsouna et al. [48] also observed a similar trend, suggesting that *S. aureus* (a gram-positive bacterium) showed greater susceptibility to the antimicrobial effects of essential oils than *E. coli* (a gram-negative bacterium). In comparison to the positive control's bacteriostatic zone diameter, it was evident that the CA nanoemulsion (1.06 ± 0.11 mm) and blank nanoemulsion (1.03 ± 0.05 mm) both displayed notable inhibitory activity against *S. aureus*. However, no significant difference was observed. This phenomenon might be influenced by the potential effects of excipients within the nanoemulsion system.

4. Conclusion

Our study optimised the formulation and preparation process of CA nanoemulsions using the nanoemulsion area ratio, transmittance, particle size, PDI, and Zeta potential as parameters. The optimal formulation and preparation processes were as follows: Cremophor EL and Tween 80 (mass ratio of 1.5:1) were used as surfactants, ethyl oleate as the oil phase, and absolute ethanol as the cosurfactant, and the specific Km value of surfactant to cosurfactant was 4, the O/S ratio was 1:9, and the prepared temperature was 30 °C. The CA nanoemulsion prepared under the above conditions presented slightly yellow, clear, and transparent, with the particle size of 15.46 ± 0.05 nm, PDI of 0.039 ± 0.002 and a Zeta potential of-1.37 ± 0.90 MV. Furthermore, the nanoemulsion exhibited commendable stability under various conditions, including centrifugation, neutral pH conditions, heating below 70 °C, and storage at both 4 °C and 25 °C for 60 d. The nanoemulsions exhibited good slow-release effect because of the release rate of CA nanoemulsions was slower than that of CA solutions. However, the bacteriostatic activity of CA nanoemulsion was not significantly better than that of blank nanoemulsion. Subsequently, an in-depth study will be conducted on this aspect. This study provides evidence that a CA nanoemulsion is valuable for enhancing solubility of CA and could potentially be used to enhance the oral absorption of poorly water-

Table 5
Bacteriostatic effect in *S. aureus* and *E. coli*.

Strain	Bacteriostatic circle diameter/mm					
	A	B	C	D	E	F
S. aureus	1.06 ± 0.11^{a}	1.03 ± 0.05^{a}	0.8 ± 0.10^{b}	1.03 ± 0.05^{a}	0.73 ± 0.07^{b}	0.9 ± 0.01^{ab}
E. coli	0.86 ± 0.11^{c}	0.76 ± 0.05^{c}	1.2 ± 0.01^{b}	1.5 ± 0.10^{a}	0.8 ± 0.10^{c}	0.8 ± 0.01^{c}

Note: "A" is a synergistic corosoic acid nanoemulsion, "B" is a blank nanoemulsion, "C" is the positive control penicillin, "D" is the positive control streptomycin, "E" is the solution of corosolic acid and "F" is the corosolic acid nanoemulsion. Data represent mean ± standard deviation (n = 3). Significant differences ($p < 0.01$) are marked as alphabets (a-c).

soluble compounds. The successful development of CA nanoemulsions has made it possible to use nanoemulsions as delivery systems for lipophilic bio-actives.

Funding

This research was supported by the China Postdoctoral Science Foundation (no. 2022M710865), the Guangxi Natural Science Foundation for Youth (2022GXNSFBA035643), the Guangzhou Postdoctoral Project Foundation, the Xinjiang research and development program project (2022B02005-3), and the Yangxi Country Science and Technology Project (No. 21011).

Ethics declarations

Review and/or approval by an ethics committee was not needed for this study because it did not involve animal or human volunteers.

Data availability statement

Data included in article/supp. material/referenced in article. No data of this study been deposited into a publicly available repository, because this is a part of research work conducted by graduate student (First authors).

CRediT authorship contribution statement

Haimei Li: Writing – original draft, Investigation, Formal analysis, Data curation. **Xinjia Tan:** Writing – original draft, Investigation, Formal analysis, Data curation. **Liyan Qin:** Writing – original draft, Software, Formal analysis, Data curation. **Mansour K. Gatasheh:** Gatasheh, Writing – review & editing, Visualization, Funding acquisition. **Lei Zhang:** Writing – review & editing, Software, Methodology, Formal analysis. **Wenmin Lin:** Writing – review & editing, Visualization, Software. **Feng Hu:** Writing – review & editing, Visualization, Resources. **Rian Yan:** Writing – review & editing, Software, Resources, Investigation. **Mariam K. Alshammri:** Writing – review & editing, Visualization, Funding acquisition. **Yingbin Shen:** Writing – review & editing, Validation, Supervision, Resources, Project administration, Methodology, Investigation, Funding acquisition, Conceptualization. **Arshad Mehmood Abbasi:** Writing – review & editing, Visualization, Software, Methodology, Conceptualization. **Jing Qi:** Writing – review & editing, Validation, Supervision, Resources, Project administration, Funding acquisition, Conceptualization.

Declaration of competing interest

The authors declare the following financial interests/personal relationships which may be considered as potential competing interests:Haimei Li reports financial support was provided by China Postdoctoral Science Foundation. Jingqi reports financial support was provided by Guangxi Natural Science Foundation for Youth. Haimei Li reports financial support was provided by Guangzhou Postdoctoral Project Foundation. Lei zhang reports financial support was provided by Xinjiang research and development program project. Feng Hu reports financial support was provided by Yangxi Country Science and Technology Project. All authors declared that they have no known competing financial interests or personal relationships that could have appeared to influence the work reported in this paper.

Acknowledgements

We acknowledge Researchers Supporting Project number (RSP2024R393), King Saud University, Riyadh, Saudi Arabia for financial assistance. Authors would like to thank Editage (www.editage.cn) for English language editing.

Appendix A. Supplementary data

Supplementary data to this article can be found online at https://doi.org/10.1016/j.heliyon.2024.e38283.

References

[1] Y. Chen, A.A. Al-Ghamdi, M.S. Elshikh, M.H. Shah, M.A. Al-Dosary, A.M. Abbasi, Phytochemical profiling, antioxidant and HepG2 cancer cells' antiproliferation potential in the kernels of apricot cultivars, Saudi J. Biol. Sci. 27 (1) (2020) 163–172, https://doi.org/10.1016/j.sjbs.2019.06.013.

[2] J. Kim, Y.H. Kim, G. Song, D. Kim, Y. Jeong, K. Liu, Y. Chung, S. Oh, Ursolic acid and its natural derivative corosolic acid suppress the proliferation of APC-mutated colon cancer cells through promotion of β-catenin degradation, Food Chem. Toxicol. 67 (2014) 87–95, https://doi.org/10.1016/j.fct.2014.02.019.

[3] G. Liu, Z. Cui, X. Gao, H. Liu, L. Wang, J. Gong, A. Wang, J. Zhang, Q. Ma, Y. Huang, G. Piao, H. Yuan, Corosolic acid ameliorates non-alcoholic steatohepatitis induced by high-fat diet and carbon tetrachloride by regulating TGF-β1/Smad 2, NF-κB, and AMPK signaling pathways, Phytother Res. 35 (2021) 5214–5226, https://doi.org/10.1002/ptr.7195.

[4] X. Qian, X. Zhang, L. Sun, W. Xing, Y. Wang, S. Sun, M. Ma, Z. Cheng, Z. Wu, C. Xing, B. Chen, Y. Wang, Corosolic acid and its structural analogs: a systematic review of their biological activities and underlying mechanism of action, Phytomedicine 91 (2021) 153696, https://doi.org/10.1016/j.phymed.2021.153696.

[5] T. Feinberg, L.S. Wieland, L.E. Miller, K. Munir, T.I. Pollin, A.R. Shuldiner, S. Amoils, L. Gallagher, M. Bahr-Robertson, C.R. D'Adamo, Polyherbal dietary supplementation for prediabetic adults: study protocol for a randomized controlled trial, Curr. Control, Trials Cardiovasc. Med. 20 (2019) 24–37, https://doi.org/10.1186/s13063-018-3032-6.

[6] J. Zhao, H. Zhou, Y. An, K. Shen, L. Yu, Biological effects of corosolic acid as an anti-inflammatory, anti-metabolic syndrome and anti-neoplasic natural compound, Oncol. Lett. 21 (2021) 84, https://doi.org/10.3892/ol.2020.12345.

[7] J. Yang, J. Leng, J. Li, J. Tang, Y. Li, B. Liu, X. Wen, Corosolic acid inhibits adipose tissue inflammation and ameliorates insulin resistance via AMPK activation in high-fat fed mice, Phytomedicine 23 (2016) 181–190, https://doi.org/10.1016/j.phymed.2015.12.018.

[8] X. Li, A.S. Widjaya, J. Liu, X. Liu, Z. Long, Y. Jiang, Cell-penetrating corosolic acid liposome as a functional carrier for delivering chemotherapeutic drugs, Acta Biomater. 106 (2020) 301–313, https://doi.org/10.1016/j.actbio.2020.02.013.

[9] H. Li, Y. Chen, Q. Peng, X. Tan, G. Chen, H. Zhou, R. Yan, Flavonoids from bamboo leaves improve the stability of unsaturated fatty acids in the lipids of walnut emulsions, Ind. Crops Prod. 178 (2022) 114609, https://doi.org/10.1016/j.indcrop.2022.114609.

[10] Z. Zeng, X. Yin, X. Wang, W. Yang, X. Liu, Synthesis of water soluble pentacyclic dihydroxyterpene carboxylic acid derivatives coupled amino acids and their inhibition activities on α-aglucosidase, Bioorg. Chem. 86 (2019) 277–287, https://doi.org/10.1016/j.bioorg.2019.02.001.

[11] Q. Huang, H. Yu, Q. Ru, Bioavailability and delivery of nutraceuticals using nanotechnology, J. Food Sci. 75 (2010) 50–57, https://doi.org/10.1111/j.1750-3841.2009.01457.x.

[12] X. Liu, Y. Lin, K. Yao, J. Xie, J. Xiao, Y. Cao, Increasing β-carotene bioavailability and bioactivity in spinach demonstrated using excipient nanoemulsions-especially those of long-chain triglycerides, Food Chem. 404 (2023) 134194, https://doi.org/10.1016/j.foodchem.2022.134194.

[13] J. Weiss, P. Takhistov, D.J. McClements, Functional materials in food nanotechnology, J. Food Sci. 71 (2006) 107–116, https://doi.org/10.1111/j.1750-3841.2006.00195.

[14] N.H.C. Marzuki, R.A. Wahab, M.A. Hamid, An overview of nanoemulsion: concepts of development and cosmeceutical applications, Biotechnol. Biotechnol. Equip. 33 (2019) 779–797, https://doi.org/10.1080/13102818.2019.1620124.

[15] G. Li, Z. Zhang, H. Liu, L. Hu, Nanoemulsion-based delivery approaches for nutraceuticals: fabrication, application, characterization, biological fate, potential toxicity and future trends, Food Funct. 12 (2021) 1933–1953, https://doi.org/10.1039/D0FO02686G.

[16] M. Miastkowska, P. Sliwa, Influence of terpene type on the release from an O/W nanoemulsion: experimental and theoretical studies, Molecules 25 (2020) 2747, https://doi.org/10.3390/molecules25122747.

[17] A. Gasa-Falcon, I. Odriozola-Serrano, G. Oms-Oliu, O. Martín-Belloso, Impact of emulsifier nature and concentration on the stability of β-carotene enriched nanoemulsions during in vitro digestion, Food Funct. 10 (2019) 713–722, https://doi.org/10.1039/C8FO02069H.

[18] F. Weigel, J. Weiss, E.A. Decker, D.J. McClements, Lutein-enriched emulsion-based delivery systems: influence of emulsifiers and antioxidants on physical and chemical stability, Food Chem. 242 (2018) 395–403, https://doi.org/10.1016/j.foodchem.2017.09.060.

[19] L. Jia, D. Zhang, Z. Li, C. Duan, Y. Wang, F. Feng, F. Wang, Y. Liu, Q. Zhang, Nanostructured lipid carriers for parenteral delivery of silybin: biodistribution and pharmacokinetic studies, Colloids Surf., B 80 (2010) 213–218, https://doi.org/10.1016/j.colsurfb.2010.06.008.

[20] T. Zhao, Y. Liu, Z. Gao, D. Gao, N. Li, Y. Bian, K. Dai, Z. Liu, Self-assembly and cytotoxicity study of PEG-modified ursolic acid liposomes, Mat. Sci. Eng. C-mater. 53 (2015) 196–203, https://doi.org/10.1016/j.msec.2015.04.022.

[21] J. Liu, Q. Wang, E. Omari-Siaw, M. Adu-Frimpong, J. Liu, X. Xu, J. Yu, Enhanced oral bioavailability of Bisdemethoxycurcumin-loaded self-microemulsifying drug delivery system: formulation design, *in vitro* and *in vivo* evaluation, Int. J. Pharm. (Amst.) 590 (2020) 119887, https://doi.org/10.1016/j.ijpharm.2020.119887.

[22] J. Luo, B. Yang, X. Yang, S. Ji, Z. Guo, Y. Liu, Q. Chen, T. Zhao, Y. Wang, B. Lu, Sophorolipid-based microemulsion delivery system: multifaceted enhancement of physicochemical properties of xanthohumol, Food Chem. 413 (2023) 135631, https://doi.org/10.1016/j.foodchem.2023.135631.

[23] M.S. Algahtani, M.Z. Ahmad, J. Ahmad, Investigation of factors influencing formation of nanoemulsion by spontaneous emulsification: impact on droplet size, polydispersity index, and stability, Bioengineering 9 (2022) 384, https://doi.org/10.3390/bioengineering9080384.

[24] N. Kumar, A. Mandal, Thermodynamic and physicochemical properties evaluation for formation and characterization of oil-in-water nanoemulsion, J. Mol. Liq. 266 (2018) 147–159, https://doi.org/10.1016/j.molliq.2018.06.069.

[25] M. Firoozi, S. Rezapour-Jahani, Z. Shahvegharasl, N. Anarjan, Ginger essential oil nanoemulsions: preparation and physicochemical characterization and antibacterial activities evaluation, J. Food Process. Eng. 43 (2020) e13434, https://doi.org/10.1111/jfpe.13434.

[26] S. Mansouri, M. Pajohi-Alamoti, N. Aghajani, B. Bazargani-Gilani, Stability and antibacterial activity of Thymus daenensis L. essential oil nanoemulsion in mayonnaise, J. Sci. Food Agric. 101 (2021) 3880–3888, https://doi.org/10.1002/jsfa.11026.

[27] R. Arora, G. Aggarwal, S.L. Harikumar, K. Kaur, C.M. Keck, Nanoemulsion based hydrogel for enhanced transdermal delivery of ketoprofen, Adv. Pharmaceut. Sci. (2014) 468456, https://doi.org/10.1155/2014/468456.

[28] J. Xu, D. Mukherjee, S. Chang, Physicochemical properties and storage stability of soybean protein nanoemulsions prepared by ultra-high pressure homogenization, Food Chem. 240 (2018) 1005–1013, https://doi.org/10.1016/j.foodchem.2017.07.077.

[29] Y. Shi, M. Zhang, K. Chen, M. Wang, Nano-emulsion prepared by high pressure homogenization method as a good carrier for Sichuan pepper essential oil: preparation, stability, and bioactivity, LWT–Food Sci. Technol. 154 (2022) 112779, https://doi.org/10.1016/j.lwt.2021.112779, 10.1208/s12249-020-01901-y.

[30] K. Hou, Y. Xu, K. Cen, C. Gao, X. Feng, X. Tang, Nanoemulsion of cinnamon essential oil Co-emulsified with hydroxypropyl-β-cyclodextrin and Tween-80: antibacterial activity, stability and slow release performance, Food Biosci. 43 (2021) 101232, https://doi.org/10.1016/j.fbio.2021.101232.

[31] J. Carpenter, V.K. Saharan, Ultrasonic assisted formation and stability of mustard oil in water nanoemulsion: effect of process parameters and their optimization, Ultrason. Sonochem. 35 (2017) 422–430, https://doi.org/10.1016/j.ultsonch.2016.10.021.

[32] M. Deng, H. Chen, L. Xie, K. Liu, X. Zhang, X. Li, Tea saponins as natural emulsifiers and cryoprotectants to prepare silymarin nanoemulsion, LWT–Food Sci. Technol. 156 (2022) 113042, https://doi.org/10.1016/j.lwt.2021.113042.

[33] L.M. Ferreira, M.H.M. Sari, V.F. Cervi, M. Gehrcke, A.V. Barbieri, V.A. Zborowski, R.C.R. Beck, C.W. Nogueira, L. Cruz, Pomegranate seed oil nanoemulsions improve the photostability and *in vivo* antinociceptive effect of a non-steroidal anti-inflammatory drug, Colloids Surf., B 144 (2016) 214–221, https://doi.org/10.1016/j.colsurfb.2016.04.008.

[34] M. Sessa, M.L. Balestrieri, G. Ferrari, L. Servillo, D. Castaldo, N. D Onofrio, F. Donsì, R. Tsao, Bioavailability of encapsulated resveratrol into nanoemulsion-based delivery systems, Food Chem. 147 (2014) 42–50, https://doi.org/10.1016/j.foodchem.2013.09.088.

[35] H. Sun, D. Luo, S. Zheng, Z. Li, W. Xu, Antimicrobial behavior and mechanism of clove oil nanoemulsion, J. Food Sci. Technol. 59 (2022) 1939–1947, https://doi.org/10.1007/s13197-021-05208-z.

[36] R. Verma, D. Kaushik, Design and optimization of candesartan loaded self-nanoemulsifying drug delivery system for improving its dissolution rate and pharmacodynamic potential, Drug Deliv. 27 (1) (2020) 756–771. https://doi:10.1080/10717544.2020.1760961. PMID: 32397771; PMCID: PMC7269045.

[37] R. Moghimi, L. Ghaderi, H. Rafati, A. Aliahmadi, D. McClements, Superior antibacterial activity of nanoemulsion of *Thymus daenensis* essential oil against *E. coli*, Food Chem. 194 (2016) 410–415, https://doi.org/10.1016/j.foodchem.2015.07.139.
[38] L. Lin, S. Asghar, L. Huang, Z. Hu, Q. Ping, Z. Chen, F. Shao, Y. Xiao, Preparation and evaluation of oral self-microemulsifying drug delivery system of Chlorophyll, Drug Dev. Ind. Pharm. 47 (6) (2021) 857–866. https://doi:10.1080/03639045.2021.1892746.
[39] R. Al-Karaki, A. Awadallah, H.M. Tawfeek, M. Nasr, Preparation, characterization and cytotoxic activity of new oleuropein microemulsion against HCT-116 colon cancer cells, Pharm. Chem. J. 53 (2020) 1118–1121, https://doi.org/10.1007/s11094-020-02133-x.
[40] S. Zhang, M. Zhang, Z. Fang, Y. Liu, Preparation and characterization of blended cloves/cinnamon essential oil nanoemulsions, LWT-Food Sci. 75 (2017) 316–322, https://doi.org/10.1016/j.lwt.2016.08.046.
[41] L. Zhao, Y. Wang, Y. Zhai, Z. Wang, J. Liu, G. Zhai, Ropivacaine loaded microemulsion and microemulsion-based gel for transdermal delivery: preparation, optimization, and evaluation, Int. J. Pharm. (Amst.) 477 (2014) 47–56, https://doi.org/10.1016/j.ijpharm.2014.10.005.
[42] P. Li, A. Ghosh, R.F. Wagner, S. Krill, Y.M. Joshi, A.T.M. Serajuddin, Effect of combined use of nonionic surfactant on formation of oil-in-water microemulsions, Int. J. Pharm. (Amst.) 288 (2005) 27–34, https://doi.org/10.1016/j.ijpharm.2004.08.024.
[43] N. Sharma, M. Bansal, S. Visht, P. Sharma, G. Kulkarni, Nanoemulsion: a new concept of delivery system, Chronicles Young Sci. 1 (2010) 2–6. https://www.researchgate.net/publication/42637348.
[44] M.F. Luana, H.M.S. Marcel, F.C. Verônica, G. Mailine, V.B. Allanna, A.Z. Vanessa, C.R.B. Ruy, W.N. Cristina, C. Letícia, Pomegranate seed oil nanoemulsions improve the photostability and in vivo antinociceptive effect of a non-steroidal anti-inflammatory drug, Colloids Surf., B 144 (2016) 214–221, https://doi.org/10.1016/j.colsurfb.2016.04.008.
[45] N. Mishra, K.S. Yadav, V.K. Rai, N.P. Yadav, Polysaccharide encrusted multilayered aano-colloidal system of andrographolide for improved hepatoprotection, AAPS PharmSciTech 18 (2017) 381–392, https://doi.org/10.1208/s12249-016-0512-4.
[46] C.F. Bagamboula, M. Uyttendaele, J. Debevere, Inhibitory effect of thyme and basil essential oils, carvacrol, thymol, estragol, linalool and p-cymene towards Shigella sonnei and S-flexneri, Food Microbiol. 21 (2004) 33–42, https://doi.org/10.1016/S0740-0020(03)00046-7.
[47] M. Gulluce, F. Sahin, M. Sokmen, H. Ozer, D. Daferera, Antimicrobialandantioxidant properties of the essential oilsandmethanol extract from Mentha longifolia L. ssplongifolia, Food Chem. 103 (2007) 1449–1456, https://doi.org/10.1016/j.foodchem.2006.10.061.
[48] A.B. Hsouna, M. Trigui, R.B. Mansour, R.M. Jarraya, M. Damak, S. Jaoua, Chemical composition, cytotoxicity effect and antimicrobial activity of Ceratonia siliqua essential oil with preservative effects against Listeria inoculated in minced beef meat, Int. J. Food Microbiol. 148 (2011) 66–72, https://doi.org/10.1016/j.ijfoodmicro.2011.04.028.